Structures 64 (2024) 106530

Contents lists available at ScienceDirect

Structures

journal homepage: www.elsevier.com/locate/structures

Two-heads brick masonry walls strengthened by basalt and glass chopped fiber mortar: Effect of bed joints and coating reinforcements

Micaela Mercuri [a,1], Marco Vailati [b,*,2], Amedeo Gregori [b]

[a] Department of Civil and Environmental Engineering, Northwestern University, Evanston, IL, USA
[b] Department of Civil, Construction-Architectural and Environmental Engineering, University of L'Aquila, Piazzale Ernesto Pontieri, Monteluco, Poggio di Roio, L'Aquila 67100, Italy

ARTICLE INFO

Keywords:
Seismic retrofitting
Bed-joints reinforcement
Glass fibers
Basalt fibers
External reinforcement
In-plane experimental test

ABSTRACT

It is urgent finding strengthening systems for masonry structures located in seismic areas. This paper studies the effect of chopped fibers embedded in a cementitious mortar to be used as a strengthening system for two-heads brick masonry panels subjected to diagonal compressive forces. The strengthening system provides the use of two types of chopped fibers dispersed in the mortar matrix, i.e. a glass fiber reinforced mortar (G_{FRM}) and a basalt fiber reinforced mortar (B_{FRM}). The retrofitting composite material is disposed in three different ways: (i) the reinforced mortar is placed within the mortar joints of masonry panel; (ii) the reinforced mortar is disposed on both external surfaces of the masonry panel, but the mortar joints are in plain mortar; (iii) the reinforced mortar is placed both within the mortar joints and as a double reinforcing system on the external surfaces of each masonry panel. Experimental results show that in all the three cases the use of fiber reinforced mortar enhances both the shear strength and the post-peak capacity of the two-heads brick masonry panel. The most suitable behavior is related to panels reinforced with mortar both within the joints and as external reinforcing system. From the comparison between G_{FRM} and B_{FRM} it is shown that the best performance is related to basalt fibers mortar, that is also the most sustainable one. Authors always recommend the use of dispersed fibers within the mortar matrix, as it stands as effective strengthening system for new and existing masonry structures, above all when they are located in areas characterized by seismic hazard.

1. Introduction

The recent seismic events underlined once again the high vulnerability of masonry structures, both in terms of existing cultural heritage, constituted by churches [1–7], palaces [8,9] and towers [10,11], and more recent buildings composing the majority of people's housing structures: finding proper methods of analysis [12], verification procedures and, above all, effective strategies for strengthening masonry systems is an urgent task for politicians, researchers and engineering practitioner [13].

Nowadays, two are the most diffused retrofitting systems for masonry structures, i.e. the fiber reinforced polymers (FRP) [14–20] and fiber reinforced cementitious matrix (FRCM) composites [21–27]. Due to the random direction of the seismic action, FRCM's are developed and applied at the structural scale to improve both the in-plane [28–33] and the out-of-plane behavior of masonry panels [34–40].

FRPs are to some extent effective in increasing the load-carrying capacity of masonry elements but, their disadvantages (as low fire resistance, low permeability, impossibility of application on wet surfaces and, above all, poor chemical compatibility with masonry supports) makes them not favorites for intervention on historical heritage. FRCMs composites are generally composed of fiber fabrics embedded in an inorganic matrix mortar [41–48]. The used fibers can be made out of steel [49–52], carbon [53–56], glass [57–60], basalt [61–65], aramid [66] and also vegetable fibers [67–69]. FRCMs showed to be able to increase the resistance to high temperatures and they have a quite good vapor permeability [70].

However, FRCM is still a limited technique for the strengthening and the restoration of the masonry structures because of its installation procedure. As a matter of fact, one of the main drawbacks of FRCM's

* Corresponding author.
E-mail address: marco.vailati@univaq.it (M. Vailati).
[1] ORCID: 0000-0002-9717-0705
[2] ORCID: 0000-0002-5515-3894

https://doi.org/10.1016/j.istruc.2024.106530
Received 13 November 2023; Received in revised form 14 March 2024; Accepted 2 May 2024
Available online 8 May 2024

comes out when the reinforcement system is extensively applied to continuous masonry structures, mainly because the application phase is almost entirely hand-made and it is a very time consuming activity. In fact, the FRCM reinforcement process for masonry panels is composed by three phases: (i) application of a first layer of mortar matrix on the masonry surface; (ii) application of the fiber reinforcement by lightly pressing the grid on the fresh mortar layer; (iii) application of a second and finishing layer of mortar, fully covering the grid and totally embedding the fibers into the inorganic matrix.

This paper proposes to use a chopped fiber reinforced mortar (denominated hereinafter FRM), composed by fibers directly embedded in the mortar matrix, for the strengthening of mortar panels. In this way, the proposed mortar can be applied all at once as a single reinforcement-finishing layer and it can even be sprayed on the existing masonry support or, alternatively, can be applied by manual lay-up to the surface of the masonry panels. In both cases, one assists to a decrease of both the building or restorations costs and the constructions times.

In particular, this study investigates the effect of both glass fiber reinforced mortars (G_{FRM}) and basalt fiber reinforced mortars (B_{FRM}) on the diagonal compressive behavior of brick masonry panels in the three following configurations: (i) the reinforced mortar is just placed within the mortar joints of masonry panel; (ii) the reinforced mortar is disposed as a double reinforcing layer on both external surfaces of the masonry panel, whereas the mortar joints are characterized just by plain mortar; (iii) the reinforced mortar is placed both within the mortar joints of masonry bricks and as a double reinforcing layer on the external surfaces of each masonry panel.

2. Material properties

In this section, the three material constituting the masonry panels will be illustrated, i.e. the masonry brick, the basalt fiber reinforced mortar and the glass fiber reinforced mortar.

2.1. Bricks

The fundamental properties of bricks were calculated by performing standard tests according to [71] and they are reported in Table 1. The coefficients of variation reported in Table 1 were computed after testing 15 bricks.

2.2. Mortar

Three different types of mortar were used in this study: (i) plain mortar, (ii) chopped glass reinforced mortar, (iii) chopped basalt fiber reinforced mortar. Aiming to analyze the effect of the type of fibers on the mechanical properties of the masonry wall, the mortar mix design, as well as the water content represent invariants during the experimental campaign and they were kept fixed for both unreinforced and reinforced mortars.

2.2.1. Plain mortar

The mix-design for the plain mortar is characterized by: aggregates composed by sand, whose size goes from 0.1 mm to 1.2 mm and whose content is equal to 65% of the total weight of the mixture; for what concerns the binders, the lime content is the 70% of the total weight of the binders, and the remaining 30% is a cementitious binder; the water content is the 80% of the weight of the binder and to the 20% of the total weight of the product. After the mix-phase carried on for 60 s, the mortar was cast in three molds (whose measures were 160 mm × 40 mm×40 mm). After 28 days the specimens were tested according to the standard code EN 1015–11 [72], in flexural configuration. For the characterization of the tensile and the compressive response, the tests were performed on 40 mm x 40 mm x 80 mm prisms obtained from one the two-half specimens representing the broken pieces of the 3PBT. Fig. 1 illustrates the testing apparatus and structural schemes the three-point bending test (3PBT), the splitting test (ST), and the compression test (CT).

Table 1
Geometrical and mechanical properties for bricks.

Property	Value (CoV in %)
Dimension (mm)	240 × 120 x 55 (1)
Compressive strength (MPa)	35 (7)
Tensile strength (MPa)	3.7 (5)
Water absorption (%)	14.8 (9)

After the 3PBT, the flexural strength σ_f can be computed with a formula inferred from the elasticity theory:

$$\sigma_f = \frac{3VL}{2b(d-a)^2} \tag{1}$$

where V is the peak vertical load, b is the depth of the specimen, d is its height, a is the crack length and L is the specimen length. After performing the ST and the CT, the tensile strength f_t and the compressive strength f_c can be computed by resorting on the following formulas:

$$f_t = \frac{2F}{\pi bd} \tag{2}$$

$$f_c = \frac{C}{bL_2} \tag{3}$$

where F and C are the peak vertical loads in tensile and compressive configuration, respectively.

For the three plain mortar cases (URM), as well as for the three GFRCM cases and the three BFRCM cases, Fig. 2a and Fig. 2b show the flexural stress σ_f and tensile stress $f_t$versus displacement δ curves, respectively. Fig. 2c reports the compressive stress f_c versus vertical strain ε_v for the same aforementioned cases.

2.2.2. Reinforced mortar: glass FRM and Basalt FRM

For all the fiber reinforced specimens, chopped fibers were included as the last step of the dry-mixing phase and prior to add water within the conglomerate. Aiming to analyze the effect of the type of fibers on the mechanical properties of brick masonry panels, the geometrical characteristics of both glass and basalt fibers were chosen to be as similar as possible. Table 2 reports the geometrical and mechanical properties of both glass and basalt fibers dispersed in the mortar matrix and Fig. 2 shows their physical and geometrical features. It is also important to point out the procedure followed for the determination of the fiber content FC within the mortar: previous studies [61,73] showed the mechanical properties of the reinforced mortar to increase, by augmenting the fiber content, for a certain fiber length FL; therefore, one can wrongly think that the most suitable fiber reinforced mortar is the one characterized by the maximum FC. However, this is not the best engineering solution, because it does not satisfy the fundamental requirement of the workability. The fulfillment of the workability ensures the mortar to be practically applied on structures (i.e. at a large scale by both normal and specialized workmanship) and, therefore, it stands as an inalienable feature. The requirement of workability can be satisfied if the slump value is not less that 15.5 mm. This value is met for a fiber content FC= 1.2% for glass fiber reinforced mortar and FC= 1.9% for basalt fiber reinforced mortar.

The characterization of the mechanical properties for the reinforced mortar followed the same procedure reported for the URM cases. Figs. 3a and 3b show the flexural stress σ_f and tensile stress f_t versus displacement δ curves, respectively, for both G_{FRM} and B_{FRM}. For the same cases, Fig. 3c illustrates the compressive strength f_c versus vertical strain ε_v.

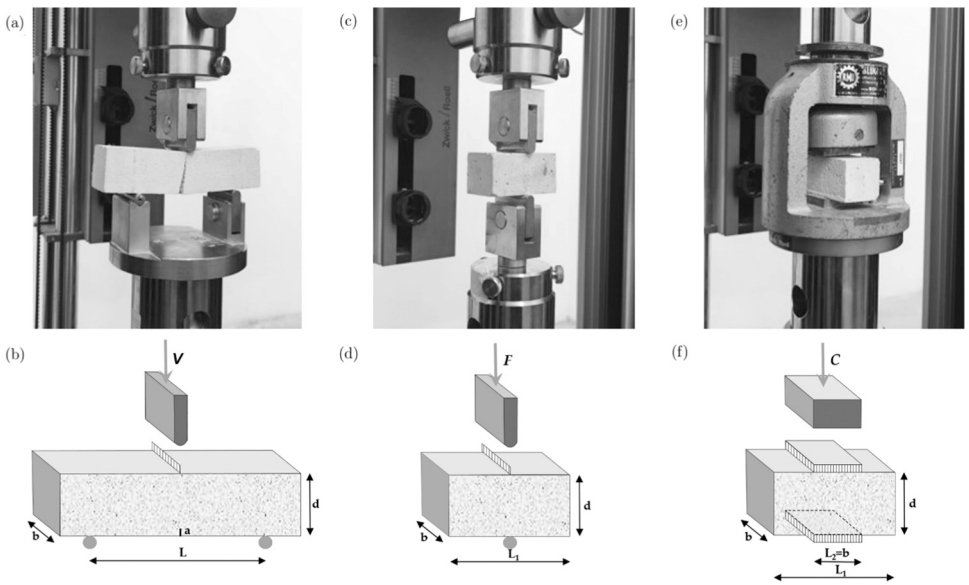

Fig. 1. Configuration of the testing apparatus and structural schemes for: a) and b) three point bending test (3PBT), c) and d) splitting test (ST), e) and f) compression test (CT).

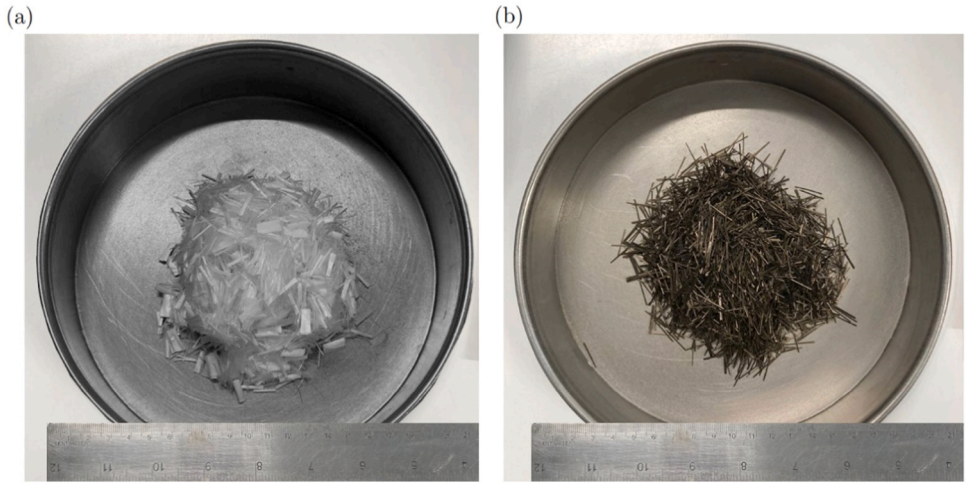

Fig. 2. (a) Chopped Glass fibers; (b) Chopped Basalt fibers.

Table 2
Geometrical and mechanical properties of fibers dispersed in the mortar matrix.

Nomenclature	l_f (mm)	d_f (mm)	ρ_f (kg/m^3)	E_f (MPa)	$f_{t,f}$ (MPa)	$\varepsilon_{u,f}$ (%)
Glass F12	12	0.0135	2680	72,000	1700	3.7
Basalt F12	12	0.04	1300	41,000	1600	6.5

Table 3
Mechanical properties of reinforced mortar, i.e. G_{FRM} and B_{FRM}.

Nomenclature	σ_f [MPa] (CoV in %)	f_t [MPa] (CoV in %)	f_c [MPa] (CoV in %)
Plain mortar prisms	2.9 (6.1)	1.9 (2.6)	17.5 (1.8)
Glass FRM prisms	11.7 (6.4)	2.4 (3.2)	23.8 (4.2)
Basalt FRM prisms	12.1 (7.4)	2.6 (9.6)	24.1 (6.0)

2.3. Experimental design

The experimental campaign aims to understand the effect of both glass and basalt-reinforced mortar (named G_{FRM} and B_{FRM}, respectively) on the diagonal-compressive and shear behaviors of brick masonry panels. In particular, the beneficial effect of the two reinforcing systems has been tested for three possible arrangements of the reinforced mortar: (i) FRMs placed just in the mortar joints, (ii) unreinforced mortar joints and FRMs arranged as an internal-external layer on the surface of the masonry panel, and (ii) FRMs placed in both mortar joints and as a superficial internal-external layer of the masonry panels. By sake of comparison, the unreinforced case (denominated URM in Table 4) was also analyzed, providing that plain mortar joints were not reinforced with any types of fibers. Fig. 4 shows a 3D structural scheme underlying the location of fiber-reinforced mortar. The first set of cases were characterized by masonry panel measuring 1000 mm × 1030 mm x 250 mm and having a uniform thickness of mortar joints equal to 10 mm. These cases are identified by URM, J-G_{FRM} and J-B_{FRM} cases in Table 4 and they are shown in Fig. 5a. In the second set of experiments, each masonry panel measures 1000 mm × 1030 mm x 290 mm and the

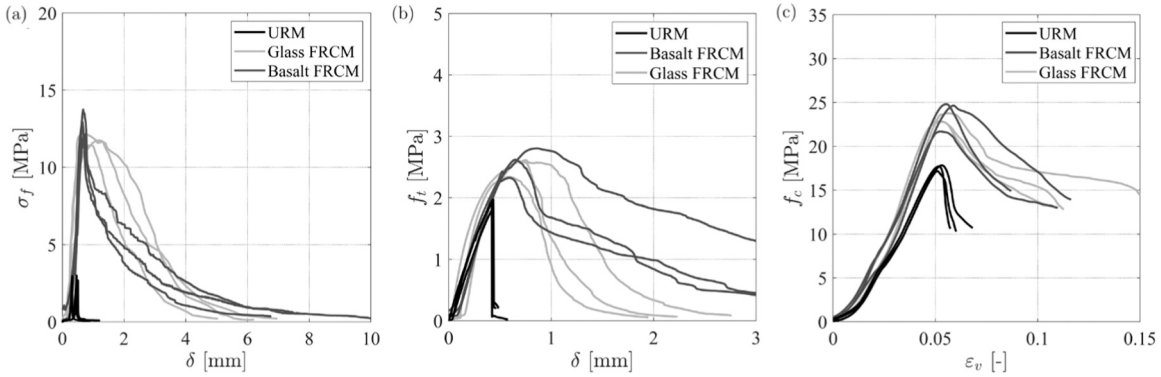

Fig. 3. (a) Flexural stress vs displacement curves; (b) Tensile stress vs displacement curves; and (c) Compressive strength vs displacement curves.

Table 4
Summary of brick masonry panels tested in diagonal-compressive configuration.

Nomenclature	Dimensions (mm)	Joint Reinforcement type	External Reinforcement type	Case set
URM	1000 × 1030 x 250	-	-	1, 2, 3
J-G_{FRM}	1000 × 1030 x 250	Glass fibers	-	1
J-$B1_{FRM}$	1000 × 1030 x 250	Basalt fibers	-	1
J-$B2_{FRM}$	1000 × 1030 x 250	Basalt fibers	-	1
C_{URM}	1000 × 1030 x 290	-	-	2
C-G_{FRM}	1000 × 1030 x 290	-	Glass fibers	2
C-B_{FRM}	1000 × 1030 x 290	-	Basalt fibers	2
JC-G_{FRM}	1000 × 1030 x 290	Glass fibers	Glass fibers	3
JC-B_{FRM}	1000 × 1030 x 290	Basalt fibers	Basalt fibers	3

out of plane dimension includes a 2 cm thickness coating referring to each reinforcement layer (a total of 40 mm as the coating was applied to both the internal and external surfaces) and these cases are denominated C_{URM}, C-G_{FRM} and C-B_{FRM} in Table 4. The third and last set of experimented panels have both reinforced joints and coating with either glass or basalt fibers and they are denominated JC-G_{FRM} and JB-G_{FRM} in Table 4, respectively. All the C-cases provide the application reinforced mortar just on the two external surfaces and the proposed reinforcement system is adapted to strengthen existing structures and new ones. On the other hand, all the J-cases provide the entire reinforcement of the mortar joints with fibers and the reinforcement system is therefore applicable just to new construction.

2.4. Test setup and loading protocol

The test apparatus and loading protocol adopted in this study followed the guidelines recommended by [74]. It is worth underlying that all panels were preliminarily rotated of 45° with respect to the horizontal axis and collocated in the Instron machine in Laboratory of Material and Structures of University of L'Aquila (IST Systems - Labtronic 8800 Structural Test Controls System), as shown in Fig. 5b. Fig. 5c shows the experimental setup for the diagonal compression test and it illustrates some details of the loading apparatus: a couple o 'V-shaped' steel elements measuring about 152 mm each side, were placed at the two panel corners and connected by two triangular steel plates, aiming to avoid the crushing-corner modality of failure. Two Linear Variable Displacement Transducers (LVDTs) are placed on each side of the panel (for a total of four transducers) to record both vertical and horizontal panel displacements. The LVDTs base length was kept constant to about 800 mm. The force was applied in displacement control conditions on the top of the vertical axis of the panel, whereas the bottom side was fixed in translations and rotations. The loading rate was about 0.5 mm/min and the piston advanced up to the complete sample failure. Data points related to both loads and displacements were recorded at a frequency equal to 5 Hz.

3. Analysis of results

3.1. Enhancement of the bearing capacity

The results are illustrated in Fig. 6, that shows the vertical load P versus vertical displacements Δv curves. It is worth observing that the presence of fiber reinforcement in the mortar joints improves the mechanical capacity of the masonry panel in diagonal compression, as shown in Fig. 6a. More precisely, the beneficial effect is more pronounced when chopped basalt fibers are used with respect to the glass fiber cases; this result appears evident if one compares the gray line in Fig. 6a, corresponding to the unreinforced panel (URM case), with the dotted blue and red lines, representing the glass and basalt joint reinforced panels (J-G_{FRM} and J-B_{FRM} cases), respectively. In particular, the peak loads related to J-B_{FRM} and J-G_{FRM} cases increase of 58.1% and 48.4% with respect to the URM case, respectively. More important role in the mechanical response of the masonry panel is played by the fiber mortar when applied as internal-external coating: in case the glass fibers are used as reinforcement (C-G_{FRM} case, marked with a continuous blue curve in Fig. 6b) the peak loads increase of 238.7% with respect to URM case and of 202.9% with respect to C_{URM} case, whereas the enhancement of the peak load reaches 259.7% with respect to URM case and of 215.7% with respect to C_{URM} case, when basalt fibers are used in the mortar matrix (C-B_{FRM} case, marked with a continuous red curve in Fig. 6b). Of course, aiming to maximize the retrofitting of brick masonry panels, the most suitable cases are the ones characterized by fiber reinforcement in both mortar joints and internal-external layer of fiber reinforced mortar, as shown in Fig. 6c. Also for this case, the best performance is the one related to the adoption of basalt fiber as reinforcement of the mortar matrix (case in Fig. 6c). In fact, the increase of the peak load reaches of 333.9% for JC-B_{FRM} case as compared with the URM case and of 274.5% with respect to C_{URM} case. On the other hand, very effective appears the use of glass fiber for this last set of cases: the peak load shows an increase of 311.3% for JC-G_{FRM} case with respect to the URM case and of 264.7% with respect to C_{URM} case.

3.1.1. Shear strength

According to [74–76], it is possible to compute the shear stress τ resorting on the following equation:

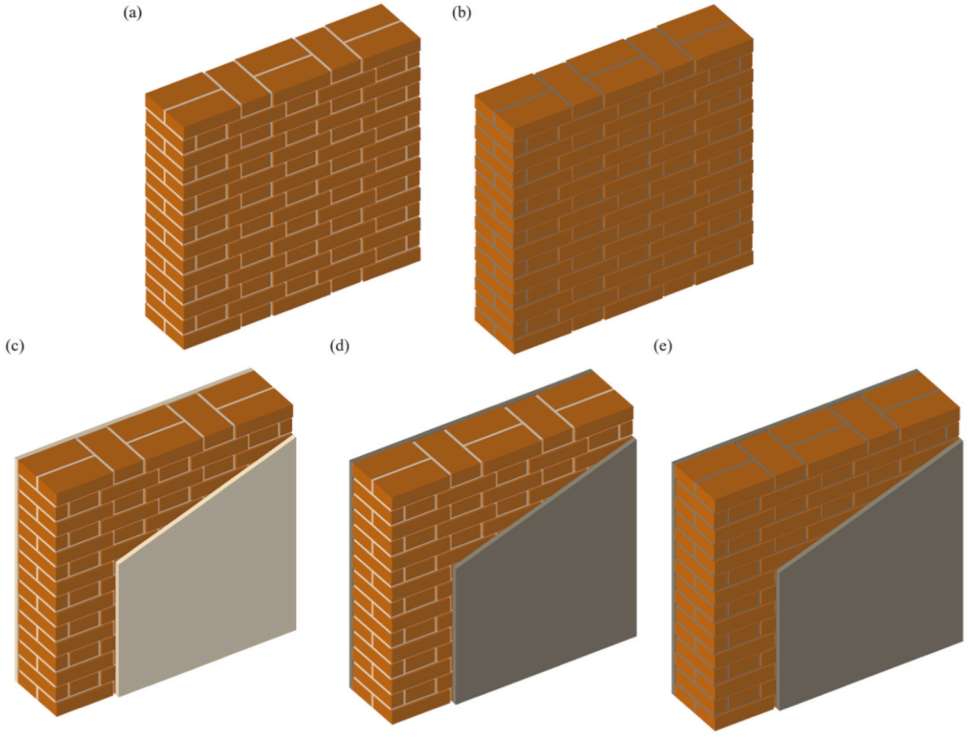

Fig. 4. (a) URM case: plain mortar placed in joints; (b) J-cases: FRM placed in mortar joints; (c) C_{URM}: plain mortar placed in mortar joints and as external coating; (d) C-cases: plain mortar joints placed in joints and FRM placed as external coating; (e) JC-cases: FRM placed in joints and as external coating.

$$\tau = \frac{0.707 \quad P}{A_n} \tag{4}$$

Where A_n is net area of the panel expressed as $A_n = (W+h)/2) * t$ and W, h, and t are the width, height, and thickness of the panel, respectively. It is important to underline that A_n is different for unreinforced and externally reinforced panels, because their thickness is different: t for is equal to 250 mm and 290 mm, for unreinforced and externally reinforced panels, respectively. When P reaches P_0, τ reaches the shear strength τ_0. To compute the deformation capacity of the panel, one can write the following equation:

$$\gamma = \frac{\Delta v + \Delta h}{g} \tag{5}$$

where Δv and Δh are the vertical and horizontal displacements measured by the LVDTs and g is the LVDT length.

The results are shown in Fig. 7, that reports the shear stress τ versus shear strain γ curves. Similar qualitative results pointed out in Fig. 6 can be underlined in Fig. 7 and they are properly related to the shearing capacity of the panels. For all the three set of cases, the fiber beneficial effect is more evident when basalt fibers are used with respect to glass fibers (comparison of red and blue curves in Fig. 7). When fibers are used in the mortar joints (J-G_{FRM} and J-B_{FRM} cases in Fig. 7a) the beneficial effect is moderate and the shear strength related to J-B_{FRM} and J-G_{FRM} cases increase of about 43% and 32% than to the URM case, respectively.

When fiber reinforced mortar is used as a double layer reinforcing (C-B_{FRM} and C-G_{FRM} cases in Fig. 7b), the shear strengths increase of 218% and 194% with respect to URM case, respectively. The optimum solution in reached when fiber reinforced mortar is used both within the joints and as an internal-external coating (JC-B_{FRM} and JC-G_{FRM} cases in Fig. 7c): in this cases the shear strengths increase of 282% and 265% with respect to URM case, respectively.

4. Improvement of the post-peak behavior

Section 3.3.1 unequivocally pointed out the improvement of the diagonal and shear bearing capacity under a quantitative point of view. The current section proves the increasing of the post peak capacity of the brick masonry panels under both a qualitative and quantitative point of view.

4.1. Fracturing pattern

The fracturing pattern is a good qualitative indicator of the post-peak capacity of most of quasi-brittle materials. Fig. 8 depicts the fracturing patterns related to the three analyzed cases characterized by reinforced mortar placed in the mortar joints (Fig. 8b), as internal-external coating (Fig. 8c) and a joints and superficial reinforcement system (Fig. 8d). In Fig. 8a, it is also reported the crack pattern related to the plain mortar case. For the case shown in Fig. 8b, one can observe that the main crack mostly follows the brick-mortar interface and it is characterized by a very jagged shape. The fracturing difference with the plain mortar case is that, in this latter case, the fracture propagates within the mortar joints rather than in correspondence of the brick-mortar interface; the physical explanation of this observation lays on the fact that plain mortar is mechanically weaker than the chopped fibers reinforced one, therefore being more prone to host the crack. In case the reinforcing mortar is used as internal-external coating, as shown in Fig. 8c, the fracturing pattern does not follow the brick-mortar interface and it is less articulated spatially: it appears as a single crack that extends from north to south of the reinforced panel. From this observation, one can infer that is the mortar coating that directs the modality of fracture, being therefore the main responsible for the increasing in the post-peak behavior. In this case, if one observes the underlined crack at the masonry level, the crack does not happen within the mortar joint, but the fracture propagates almost straight north to south, thus affecting both bricks and mortar joints, alternatively. This is shown in Fig. 8e. The last case is shown in Fig. 8d, pointing out that the fracture path is very

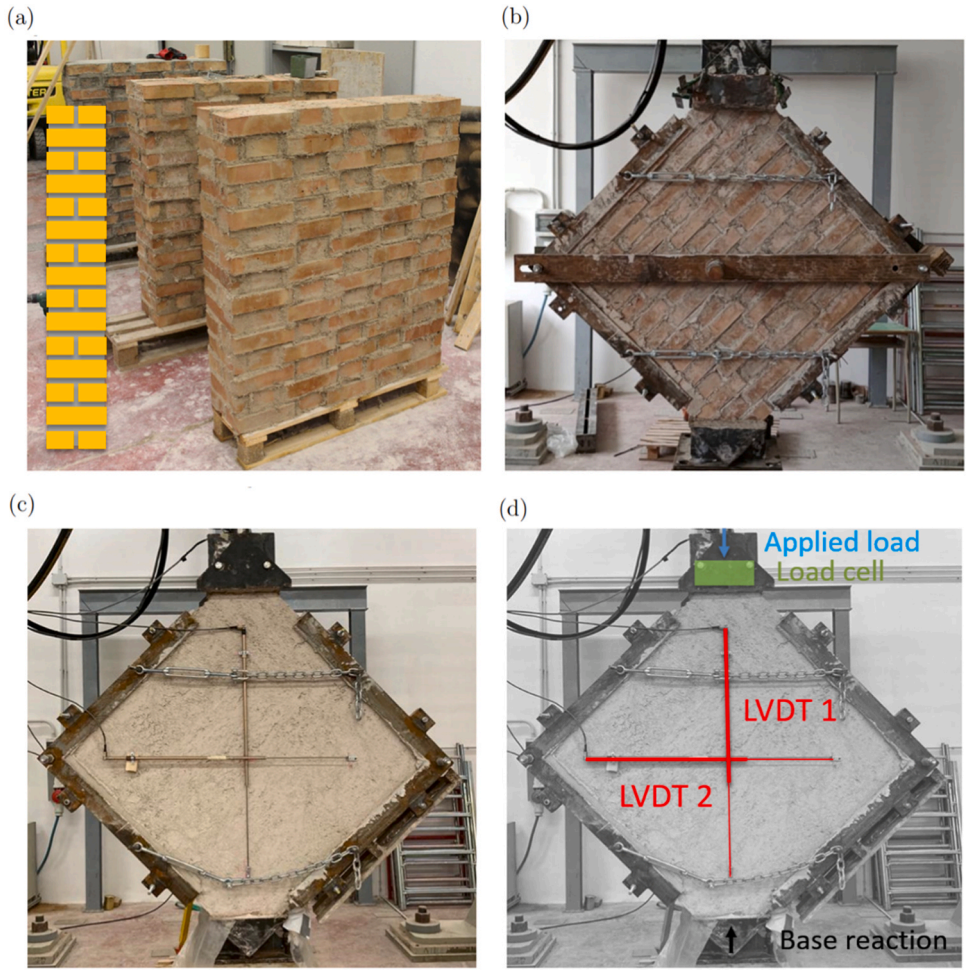

Fig. 5. (a) Preparation of experimental panels (J-G_{FRM}, J-$B1_{FRM,}$ J-$B2_{FRM}$) and sectional scheme of the two head masonry panel; (b) panel rotation of 45° with respect to the horizontal axis and its collocation in the Instron machine in Laboratory of Material and Structures of University of L'Aquila; (c) placement of two Linear Variable Displacement Transducers (LVDTs) on each side of the panel to measure the vertical and horizontal panel displacements; (d) scheme of the experimental setup.

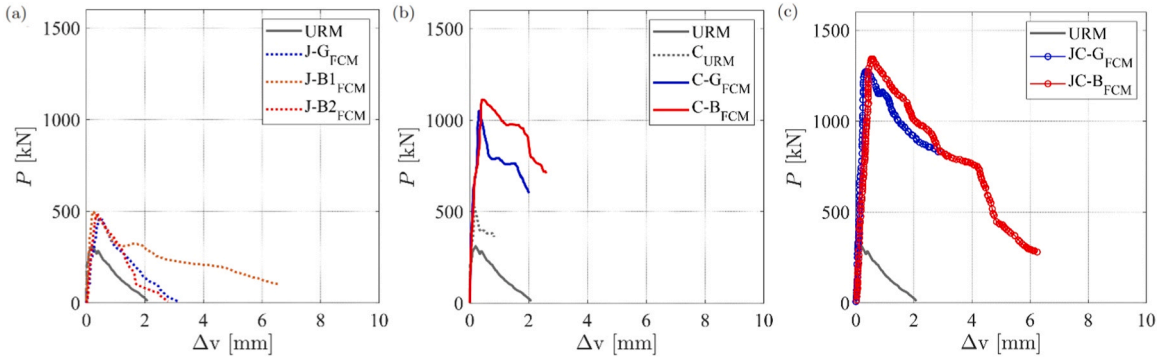

Fig. 6. Load P versus vertical displacements Δv curves for cases with reinforced mortar placed in: (a) mortar joints; (b) as internal-external coating; (c) both mortar joints and internal-external coating.

articulated when reinforced mortar is used both as a surface coating and a joints reinforcement. In this case, there is the coalescence of several micro- and meso-cracks oriented in the vertical direction of the masonry panels. This fact indicates that there are two antagonist mechanical processes that are competing: the joints reinforcement directs the fracture within the brick-mortar interface, whereas the superficial reinforcement orients the single crack in the north-south direction. The overall results can be seen as a superposition of both the strengthening effects.

4.2. Pseudo-ductility

The ductility is the material capacity to deform beyond the elastic range with a gradual drop in capacity [77]. Resorting on this feature is essential while the structure responds to seismic events and this capacity is quantitatively considered by many seismic based design codes [78,

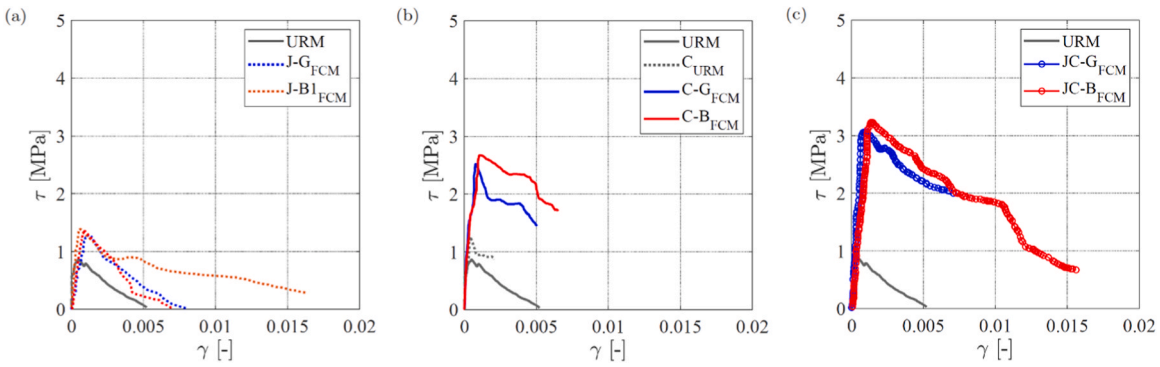

Fig. 7. Shear stress τ versus shear strain γ curves for cases with reinforced mortar placed in: (a) mortar joints; (b) as internal-external coating; (c) both mortar joints and internal-external coating.

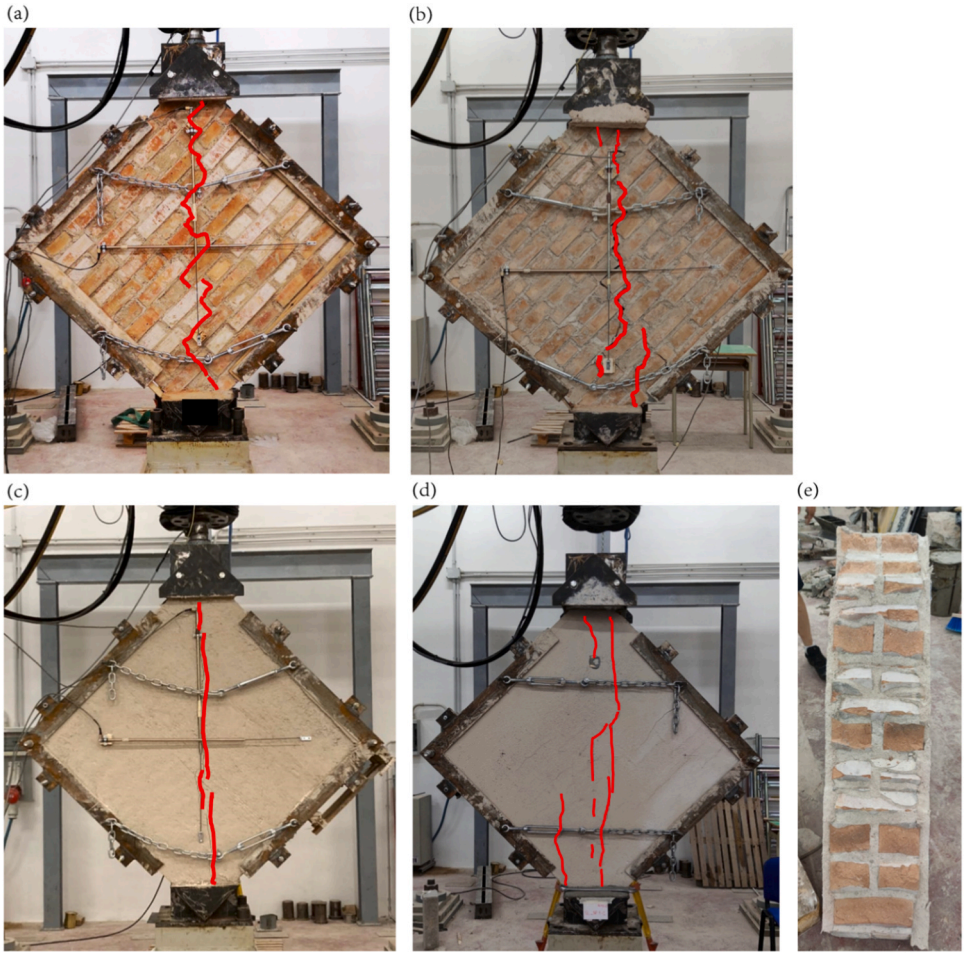

Fig. 8. Fracturing pattern for cases with reinforced mortar placed in: (a) nowhere, just plain mortar; (b) mortar joints; (c) as internal-external coating; (d) both mortar joints and internal-external coating; (e) shape of crack inside the masonry in case mortar is reinforced at both the internal and external coating (case C).

79]. In this study, the shear stress-strain plots did not show a distinct yield point and, therefore, the pseudo-ductility was determined resorting on an elasto-perfectly plastic constitutive behavior, considering: (i) for the ultimate strain γ_u the shear strain correspondent to a shear strength degraded to $0.8\tau_0$ and (ii) for the yield strain γ_y the shear strain was determined such that the area under the bilinear curve was the same as that under the experimental one. Then, the pseudo-ductility was determined by mean of the following equation:

$$\mu = \frac{\gamma_u}{\gamma_y} \tag{8}$$

Table 5 reports the values of the pseudo-ductility for all the experimented panels. First, it is worth observing that basalt chopped FRM solution is the one that most improves the pseudo-ductility for all cases. The second observation is related to the fact that applying reinforced mortar as superficial coating is more effective than the case it is applied as a joint strengthening system. This observation is true for both the glass and basalt fiber cases. Last, the solution that most enhances the pseudo-ductility is the one providing the application of basalt fiber reinforced mortar in both the joints and as an internal-external coating.

Table 5
Pseudo-ductility for all the experimented panels.

Nomenclature	Yield strain γ_y	Ultimate strain γ_u	Pseudo-ductility μ
URM	0.0010	0.0020	2.00
J-G_{FRM}	0.0015	0.0033	2.20
J-$B1_{FRM}$	0.0012	0.0045	3.75
J-$B2_{FRM}$	0.0013	0.0035	2.69
C_{URM}	0.0010	0.0021	2.10
C-G_{FRM}	0.0011	0.0037	3.36
C-B_{FRM}	0.0017	0.0062	3.64
JC-G_{FRM}	0.0014	0.0048	3.42
JC-B_{FRM}	0.0018	0.0067	3.72

5. Comparison with analytical models

This section aims to compare the experimental results with the corresponding values derived by the application of the standards for the assessment of the shear capacity of masonry panels. The analytical value of the shear stress $\boldsymbol{\tau_0}$ was evaluated by resorting on [82], that proposes to evaluate the properties of the masonry panel based on the properties of the constituent materials, i.e. bricks and mortar. By linearly interpolating the values proposed in Table 11.10. VI of [82], a mean compressive strength of the masonry panel was computed to be equal to 10.85 MPa. The second step consists in determining a range in which the shear strength is included (between $\boldsymbol{\tau_{01}}$ and $\boldsymbol{\tau_{02}}$), by referring to Tab. C8.5. I and Tab. C8.5. II in [82] and considering a masonry typology composed by solid bricks and an hydraulic lime-based mortar. The calculated shear strength range is included between 0.104 MPa and 0.221 MPa. By using the upper bound of this range, one can compute the ratio between $\boldsymbol{\tau_{0EXP}}$ and $\boldsymbol{\tau_{02}}$, as reported in Table 6. Many observations can be pointed out from this table. The most relevant is that the shear stress value derived from tests on the URM wall is 3.62 times the value obtained from the standard code, that underlines the very large safety margins guaranteed by the standards in absence of more accurate experimental tests. An other observation is related to the impossibility of increasing the theoretical shear stress resorting on the contribution of the superficial mortar coating, both in the unreinforced and fiber reinforced cases. A necessary improvement of the code is therefore related to the possibility of accounting for the beneficial contribution of coating mortar in both the unreinforced and fiber reinforced situations. This aspect is fundamental as it can impair the accuracy of the prediction and codes should be urgently updated in this direction. It is worth underlying that the experimental campaign provided the analyses of one or two panels for each reinforced structural configuration. Therefore, any regression or statistical analyses should be performed carefully, not having available a statistical significant number of tested samples.

6. Future work

Authors believe it is worth investigating in the future the following topics, on the base of the results obtained in the current study. This paper shows the beneficial effects of chopped fiber mortar on two-heads masonry brick panels. One-head masonry panels should also be studied, as several masonry infills are composed by two independent one-head masonry panels. These experimental studies should also be extended to provide simplified analytical tools to practitioner engineers and political stakeholders. Gregori and coworkers investigated the effect on the in plane behavior of brick masonry walls characterized by the presence of geometrical and material defects [80]. Masonry panels were in that case composed by unreinforced mortar. The study could be extended to understand how the presence of defects affects the in plane response of masonry bricks reinforced with chopped fiber mortar. Vailati and coworkers proposed to introduce flexible dissipative joints in two head masonry panels tested in the in plane behavior [81]. Authors would like to investigate the combined effect and dissipative joints and mortar reinforced with different chopped fibers.

Table 6
Increments of experimental shear strength with respect to Italian Standard values [82].

Nomenclature	τ_{0EXP} (MPa)	$\frac{\tau_{0EXP}}{\tau_{02}}$ (–)
URM	0.80	3.62
J-G_{FRM}	1.15	5.20
J-$B1_{FRM}$	1.25	5.66
J-$B2_{FRM}$	1.30	5.88
C_{URM}	1.90	8.60
C-G_{FRM}	2.90	13.12
C-B_{FRM}	3.05	13.80
JC-G_{FRM}	3.55	16.06
JC-B_{FRM}	3.85	17.42

7. Conclusions

This paper investigates the diagonal shear behavior of two-heads brick masonry panels strengthened by basalt or glass fiber reinforced mortar. The mortar is applied in three different configurations, i.e. (i) within the mortar joints of masonry panel, (ii) on both external surfaces of the masonry panel; (iii) both within the mortar joints and on the external surfaces of the panel.

Based on the obtained results, the following conclusions can be drawn:

- when fibers are used in the mortar joints, the beneficial effect is moderate and the shear strength increases of about 43 % and 32 % (for basalt and glass fiber reinforced mortar, respectively) with respect to the unreinforced case.
- when fiber reinforced mortar is used as a double layer reinforcing, the shear strength increase of about 218 % and 194 % (for basalt and glass fiber reinforced mortar, respectively) with respect to unreinforced case.
- the optimum solution in reached when fiber reinforced mortar is used both within the joints and as an internal-external coating: in this cases the shear strengths increase of about 282 % and 265 % (for basalt and glass fiber-reinforced mortar, respectively) with respect to unreinforced case.
- the use of fiber reinforced mortar produces an enhancement of the post-peak capacity: if fibers are used in the mortar joints the pseudo-ductility increases of about 10 % and 88 % (for glass and basalt fiber-reinforced mortar, respectively); if fiber mortar is used as reinforcement of the external surfaced the pseudo-ductility augments of about 68 % and 82 %; when both of this reinforcement strategy are used contemporaneously, the pseudo-ductility enhances of about 71% and 86 %.

Overall, authors always advice to use chopped fiber-reinforced mortar as strengthening system of new and existing masonry structures, above all when they are located in areas characterized by seismic hazard.

8. CRediT authorship contribution statement

Marco Vailati: Conceptualization, Data curation, Validation, Formal analysis, Investigation, Methodology, Writing – review & editing. **Amedeo Gregori:** Funding acquisition, Investigation, Resources. **Micaela Mercuri:** Conceptualization, Data curation, Formal analysis, Investigation, Methodology, Project administration, Supervision, Validation, Visualization, Writing – original draft, Writing – review & editing.

Declaration of Competing Interest

The authors declare that they have no known competing financial interests or personal relationships that could have appeared to influence the work reported in this paper.

Acknowledgement

The authors would also thank technicians Edoardo Ciuffitelli and Alfredo Peditto of the Laboratory of Material and Structures of University of L'Aquila.

References

[1] Lagomarsino S, Podestà S. Damage and vulnerability assessment of churches after the 2002 Molise, Italy, earthquake. Earthq Spectra 2004;20:271–83.
[2] Mercuri M, Pathirage M, Gregori A, Cusatis G. Masonry vaulted structures under spreading supports: analyses of fracturing behavior and size effect. J Build Eng 2022;45:103396.
[3] Cattari S, Resemini S, Lagomarsino S. Modelling of vaults as equivalent diaphragms in 3D seismic analysis of masonry buildings. In Structural Analysis of Historic Construction: Preserving Safety and Significance, Two Volume Set. CRC Press; 2008. p. 537–44.
[4] Mercuri M, Pathirage M, Gregori A, Cusatis G. Influence of self-weight on size effect of quasi-brittle materials: generalized analytical formulation and application to the failure of irregular masonry arches. Int J Fract 2023:1–28.
[5] D'Altri AM, Castellazzi G, de Miranda S, Tralli A. Seismic-induced damage in historical masonry vaults: a case-study in the 2012 Emilia earthquake-stricken area. J Build Eng 2017;13:224–43.
[6] D'Altri, A.M., De Miranda, S., Castellazzi, G., Sarhosis, V., Hudson, J., Theodossopoulos, D. (2019). Historic barrel vaults undergoing differential settlements. International Journal of Architectural Heritage.
[7] Mercuri M, Pathirage M, Gregori A, Cusatis G. Fracturing and collapse behavior of masonry vaulted structures: a lattice-discrete approach. Procedia Struct Integr 2023;44:1276–83.
[8] Vailati M, Monti G, Khazna MJ, Napoli A, Realfonzo R. Probabilistic assessment of masonry building clusters. Proc 15th WCEE-World Conf Earthq Eng 2012, September:1.
[9] Lagomarsino S. On the vulnerability assessment of monumental buildings. Bull Earthq Eng 2006;4:445–63.
[10] Mercuri M, Pathirage M, Gregori A, Cusatis G. On the collapse of the masonry Medici tower: an integrated discrete-analytical approach. Eng Struct 2021;246:113046.
[11] Mercuri M, Pathirage M, Gregori A, Cusatis G. Analysis of the behavior of the masonry medici tower resorting on a hybrid discrete-kinematic methodology. Procedia Struct Integr 2023;44:1640–7.
[12] Gregori A, Castoro C, Di Natale A, Mercuri M, Di Giampaolo E. Using commercial UHF-RFID wireless tags to detect structural damage. Procedia Struct Integr 2023;44:1586–93.
[13] Feilden BM, Jokilehto J. Management guidelines for world cultural heritage sites. 1998 Hist Cities: Issues Urban Conserv 2019;8:425.
[14] Triantafillou TC. Strengthening of masonry structures using epoxy-bonded FRP laminates. J Compos Constr 1998;2(2):96–104.
[15] Valluzzi MR, Tinazzi D, Modena C. Shear behavior of masonry panels strengthened by FRP laminates. Constr Build Mater 2002;16(7):409–16.
[16] Tumialan JG, Micelli F, Nanni A. Strengthening of masonry structures with FRP composites. Struct 2001 A Struct Eng Odyssey 2001:1–8.
[17] Carloni C, Subramaniam KV. FRP-masonry debonding: numerical and experimental study of the role of mortar joints. J Compos Constr 2012;16(5):581–9.
[18] Foraboschi P. Effectiveness of novel methods to increase the FRP-masonry bond capacity. Compos Part B Eng 2016;107:214–32.
[19] Grande E, Milani G, Sacco E. Modelling and analysis of FRP-strengthened masonry panels. Eng Struct 2008;30(7):1842–60.
[20] Marcari G, Manfredi G, Prota A, Pecce M. In-plane shear performance of masonry panels strengthened with FRP. Compos Part B: Eng 2007;38(7-8):887–901.
[21] D'Ambrisi A, Feo L, Focacci F. Experimental and analytical investigation on bond between Carbon-FRCM materials and masonry. Compos Part B: Eng 2013;46:15–20.
[22] Carozzi FG, Milani G, Poggi C. Mechanical properties and numerical modeling of Fabric Reinforced Cementitious Matrix (FRCM) systems for strengthening of masonry structures. Compos Struct 2014;107:711–25.
[23] Maddaloni G, Cascardi A, Balsamo A, Di Ludovico M, Micelli F, Aiello MA, et al. Confinement of full-scale masonry columns with FRCM systems. Key Eng Mater 2017;Vol. 747:374–81 (Trans Tech Publications Ltd).
[24] Bellini A, Incerti A, Bovo M, Mazzotti C. Effectiveness of FRCM reinforcement applied to masonry walls subject to axial force and out-of-plane loads evaluated by experimental and numerical studies. Int J Archit Herit 2018;12(3):376–94.
[25] D'Ambra C, Lignola GP, Prota A. Simple method to evaluate FRCM strengthening effects on in-plane shear capacity of masonry walls. Constr Build Mater 2021;268:121125.
[26] Ferretti F, Mazzotti C. FRCM/SRG strengthened masonry in diagonal compression: experimental results and analytical approach proposal. Constr Build Mater 2021;283:122766.
[27] Castori G, Corradi M, Sperazini E. Full size testing and detailed micro-modeling of the in-plane behavior of FRCM–reinforced masonry. Constr Build Mater 2021;299:124276.
[28] Mazzotti C, Ferretti F, Ferracuti B, Incerti A. Diagonal compression tests on masonry panels strengthened by FRP and FRCM. In Structural analysis of historical constructions: Anamnesis, diagnosis, therapy, controls. CRC Press; 2016. p. 1069–76.
[29] D'Antino T, Carozzi FG, Poggi C. Diagonal compression of masonry walls strengthened with composite reinforced mortar. In Key Engineering Materials, Vol. 817. Trans Tech Publications Ltd; 2019. p. 528–35.
[30] Sagar SL, Singhal V, Rai DC, Gudur P. Diagonal shear and out-of-plane flexural strength of fabric-reinforced cementitious matrix–strengthened masonry walletes. J Compos Constr 2017;21(4):04017016.
[31] Babaeidarabad S, Nanni A. In-plane behavior of unreinforced masonry walls strengthened with fabric-reinforced cementitious matrix (FRCM). Acids Spec Publ 2015;299:69–80.
[32] Crisci G, Ceroni F, Lignola GP. Comparison between design formulations and numerical results for in-plane FRCM-strengthened masonry walls. Appl Sci 2020;10(14):4998.
[33] Del Zoppo M, Di Ludovico M, Balsamo A, Prota A. Experimental in-plane shear capacity of clay brick masonry panels strengthened with FRCM and FRM composites. J Compos Constr 2019;23(5):04019038.
[34] D'Ambra C, Lignola GP, Prota A, Fabbrocino F, Sacco E. FRCM strengthening of clay brick walls for out of plane loads. Compos Part B: Eng 2019;174:107050.
[35] Ismail N, El-Maaddawy T, Khattak N, Walsh KQ, Ingham JM. Out-of-plane behaviour of in-plane damaged masonry infills strengthened using fibre reinforced matrix. 10th Int Mason Conf 2018, July:9–11.
[36] Mercuri M, Pathirage M, Gregori A, Cusatis G. Computational modeling of the out-of-plane behavior of unreinforced irregular masonry. Eng Struct 2020;223:111181.
[37] Mercuri M, Pathirage M, Gregori A, Cusatis G. Lattice discrete modeling of out-of-plane behavior of irregular masonry. Proc 8th ECCOMAS Themat Conf Comput Methods Struct Dyn Earthq Eng 2021:546–62.
[38] Scacco J, Ghiassi B, Milani G, Lourenço PB. A fast modeling approach for numerical analysis of unreinforced and FRCM reinforced masonry walls under out-of-plane loading. Compos Part B: Eng 2020;180:107553.
[39] D'Antino T, Carozzi FG, Colombi P, Poggi C. Out-of-plane maximum resisting bending moment of masonry walls strengthened with FRCM composites. Compos Struct 2018;202:881–96.
[40] Bellini A, Incerti A, Bovo M, Mazzotti C. Effectiveness of FRCM reinforcement applied to masonry walls subject to axial force and out-of-plane loads evaluated by experimental and numerical studies. Int J Archit Herit 2018;12(3):376–94.
[41] de Carvalho Bello CB, Cecchi A, Meroi E, Oliveira DV. Experimental and numerical investigations on the behaviour of masonry walls reinforced with an innovative sisal FRCM system. In Key Engineering Materials, Vol. 747. Trans Tech Publications Ltd; 2017. p. 190–5.
[42] Casacci S, Gentilini C, Di Tommaso A, Oliveira DV. Shear strengthening of masonry wallettes resorting to structural repointing and FRCM composites. Constr Build Mater 2019;206:19–34.
[43] Crisci G, Ceroni F, Lignola GP. Efficiency of FRCM systems for strengthening of masonry walls. In AIP Conference Proceedings, Vol. 2293. AIP Publishing LLC,; 2020, November, 240008.
[44] Codispoti R, Oliveira DV, Olivito RS, Lourenço PB, Fangueiro R. Mechanical performance of natural fiber-reinforced composites for the strengthening of masonry. Compos Part B: Eng 2015;77:74–83.
[45] Mercedes L, Bernat-Maso E, Gil L. In-plane cyclic loading of masonry walls strengthened by vegetal-fabric-reinforced cementitious matrix (FRCM) composites. Eng Struct 2020;221:111097.
[46] Incerti A, Tilocca AR, Bellini A, Savoia M. In-plane behaviour of FRCM-strengthened masonry panels. In Brick and Block Masonry-From Historical to Sustainable Masonry. CRC Press; 2020. p. 313–21.
[47] Cucuzza R, Domaneschi M, Camata G, Marano GC, Formisano A, Brigante D. FRCM retrofitting techniques for masonry walls: a literature review and some laboratory tests. Procedia Struct Integr 2023;44:2190–7.
[48] Ferretti F, Khatiwada S, Incerti A, Giacomin G, Tomaro F, De Martino V, et al. Structural strengthening of masonry elements by reinforced repointing combined with FRCM and CRM. Procedia Struct Integr 2023;44:2254–61.
[49] Swamy RN, Bahia HM. The effectiveness of steel fibers as shear reinforcement. Concr Int 1985;7(3):35–40.
[50] Maage M. Interaction between steel fibers and cement based matrixes. Matér Et Constr 1977;10:297–301.
[51] Sneed LH, Verre S, Carloni C, Ombres L. Flexural behavior of RC beams strengthened with steel-FRCM composite. Eng Struct 2016;127:686–99.
[52] Ombres L, Verre S. Masonry columns strengthened with Steel Fabric Reinforced Cementitious Matrix (S-FRCM) jackets: experimental and numerical analysis. Measurement 2018;127:238–45.
[53] Morgan P. Carbon Fibers and Their Composites. CRC press; 2005.
[54] Faleschini F, Zanini MA, Hofer L, Pellegrino C. Experimental behavior of reinforced concrete columns confined with carbon-FRCM composites. Constr Build Mater 2020;243:118296.
[55] Carozzi, F.G., Bellini, A., D'Antino, T., de Felice, G., Focacci, F., Hojdys, L. et al., 2017. Experimental investigation of tensile and bond properties of Carbon-FRCM composites for strengthening masonry elements. Composites Part B: Engineering, 128, p. 100–119.

[56] D'Ambrisi A, Focacci F, Luciano R, Alecci V, De Stefano M. Carbon-FRCM materials for structural upgrade of masonry arch road bridges. Compos Part B: Eng 2015;75:355–66.
[57] D'Antino T, Poggi C. Stress redistribution in glass fibers of G-FRCM composites. In Key Engineering Materials, Vol. 817. Trans Tech Publications Ltd; 2019. p. 520–7.
[58] Žmindák M, Dudinský M. Computational modelling of composite materials reinforced by glass fibers. Procedia Eng 2012;48:701–10.
[59] D'Antino T, Pellegrino C, Carloni C, Sneed LH, Giacomin G. Experimental analysis of the bond behavior of glass, carbon, and steel FRCM composites. In Key engineering materials, Vol. 624. Trans Tech Publications Ltd; 2015. p. 371–8.
[60] Donnini J, Chiappini G, Lancioni G, Corinaldesi V. Tensile behaviour of glass FRCM systems with fabrics' overlap: experimental results and numerical modeling. Compos Struct 2019;212:398–411.
[61] Ralegaonkar R, Gavali H, Aswath P, Abolmaali S. Application of chopped basalt fibers in reinforced mortar: a review. Constr Build Mater 2018;164:589–602.
[62] Jiang CH, McCarthy TJ, Chen D, Dong QQ. Influence of basalt fiber on performance of cement mortar. In Key Engineering Materials, Vol. 426. Trans Tech Publications Ltd,; 2010. p. 93–6.
[63] Chen H, Xie C, Fu C, Liu J, Wei X, Wu D. Orthogonal Analysis on Mechanical Properties of Basalt–Polypropylene Fiber Mortar. Materials 2020;13(13):2937.
[64] Pehlivan AO. Investigation of fracture parameters of concrete incorporating basalt fibers. Rev Romana De Mater 2021;51(2):247–55.
[65] Palme, J., 2014. Investigation of the Addition of Basalt Fibres into Cement.
[66] Caggegi C, Carozzi FG, De Santis S, Fabbrocino F, Focacci F, Hojdys Ł, et al. Experimental analysis on tensile and bond properties of PBO and aramid fabric reinforced cementitious matrix for strengthening masonry structures. Compos Part B Eng 2017;127:175–95.
[67] de Carvalho Bello CB, Boem I, Cecchi A, Gattesco N, Oliveira DV. Experimental tests for the characterization of sisal fiber reinforced cementitious matrix for strengthening masonry structures. Constr Build Mater 2019;219:44–55.
[68] Cristaldi G, Latteri A, Recca G, Cicala G. Composites based on natural fibre fabrics. Woven Fabr Eng 2010;17:317–42.
[69] Vailati M, Mercuri M, Angiolilli M, Gregori A. Natural-fibrous lime-based mortar for the rapid retrofitting of heritage masonry buildings. Fibers 2021;9(11):68.
[70] Bisby, L., Stratford, T., Hart, C., Farren, S.,2013. Fire performance of well-anchored TRM, FRCM and FRP flexural strengthening systems. Advanced Composites in Construction; Network Group for Composites in Construction: Chesterfield, UK, 113.
[71] 2015. Specification for Masonry Units. Clay Masonry Units. BS EN 771–1:2011+A1:2015, British Standard.
[72] European Committee of Standardization (CEN) 1999, 'Methods of test for mortar for masonry – Part 11: Determination of flexural and compressive strength of hardened mortar', EN 1015–11,Brussels, August 1999.
[73] Mercuri M, Vailati M, Gregori A. Lime-based mortar reinforced with randomly oriented polyvinyl-alcohol (PVA) fibers for strengthening historical masonry structures. Dev Built Environ 2023;14:100152.
[74] American society for testing material - ASTM. (2021). E519/ E519M. Standard Test Method For Diagonal Tension (Shear) In Masonry Assemblages. ASTM International.
[75] Borri A, Castori G, Corradi M, Speranzini E. Shear behavior of unreinforced and reinforced masonry panels subjected to in situ diagonal compression tests. Constr Build Mater 2011;25(12):4403–14.
[76] Ismail N, Petersen RB, Masia MJ, Ingham JM. Diagonal shear behaviour of unreinforced masonry wallettes strengthened using twisted steel bars. Constr Build Mater 2011;25(12):4386–93.
[77] Giberson MF. Two nonlinear beams with definitions of ductility. J Struct Div 1969;95(2):137–57.
[78] Fardis MN. Capacity design: early history. Earthq Eng Struct Dyn 2018;47(14):2887–96.
[79] Magenes, G., & Penna, A. (2011, February). Seismic design and assessment of masonry buildings in Europe: recent research and code development issues. In Proceedings of the 9th Australasian masonry conference (Vol. 15, p. 18). Queenstown, New Zealand: Australian Masonry Conference, Auckland. [80] Ismail, N., Petersen, R. B., Masia, M.
[80] Gregori A, Mercuri M, Angiolilli M, Pathirage M. Simulating defects in brick masonry panels subjected to compressive loads. Eng Struct 2022;263:114333.
[81] Vailati M, Gregori A, Mercuri M, Monti G. A non-intrusive seismic retrofitting technique for masonry infills based on bed-joint sliding. J Build Eng 2023;69:106208.
[82] NTC 2018. 'Norme Tecniche per le Costruzioni', Ministery of the Infrastractures and Transports of the Italian Republic, decree 17 Jan. 2018.